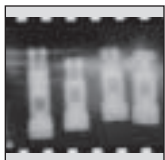# Nonceramic Hydroxyapatite Bone Derivative in Sinus Augmentation Procedures: Clinical and Histomorphometric Observations in 10 Consecutive Cases

Zvi Artzi, DMD*
Carlos E. Nemcovsky, DMD*
Dan Dayan, DMD, MSc**

A synthetic, nonceramic resorbable hydroxyapatite (R-HA) was applied to augment the subantral area in 10 consecutive sinus lift procedures in humans. Implants were simultaneously placed in eight patients; in the remaining two, where residual bone height was less than 3 mm, a two-stage surgical approach was carried out. The aim of the study was to examine, clinically and histopathologically at 12 months, the healing pattern of these augmented sinuses around the implants. In the simultaneous technique, radiopaque grafted mineral surrounded the implants. In the two-stage technique, R-HA particles filled the augmented site and were confined to the subantral area. At the uncovering phase, all implants (n = 36) were stable, with no clinical bone resorption around the cervix. A 2.5-mm trephine bur was used to collect specimens from the 10 augmented sites at the lateral-deep area. Histologically, new bone formation was evident in all examined cores. R-HA particles were primarily surrounded by newly formed bone, mostly woven bone, in different stages of remodeling. However, in the deep areas of the specimen cores, lamellar bone fragments were also seen. Morphometric measurements showed that the mean bone area of the 10 sites was 28.1% at the lateral/external side and 37.8% at the deep/inward side. Under polarizing microscopy, the mean lamellar:woven bone ratio was 1:7.2 at the lateral side and 1:4.2 at the deep end. Differences were statistically significant. R-HA proved to be a suitable filler material for osseointegrated implants in sinus augmentation procedures, since it showed both biocompatible and osteoconductive properties. (Int J Periodontics Restorative Dent 2003;23:381–389.)

 *Senior Lecturer, Department of Periodontology, The Maurice and Gabriela Goldschleger School of Dental Medicine, Tel Aviv University, Israel.
**Associate Professor, Department of Oral Pathology and Oral Medicine, The Maurice and Gabriela Goldschleger School of Dental Medicine, Tel Aviv University, Israel.

Reprint requests: Dr Zvi Artzi, Department of Periodontology, The Maurice and Gabriela Goldschleger School of Dental Medicine, Tel Aviv University, Tel Aviv, Israel. Fax: + 972-3-6409250. e-mail: zviartzi@post.tau.ac.il

Subantral floor augmentation and simultaneous or delayed implant placement have become predictable procedures in prosthetic reconstruction of atrophic posterior maxillae. Several different bone substitutes have been used to augment the sinus floor area.[1–7] Biocompatibility and osteoconductivity have been found in various calcium phosphate alloplasts.[8–10] A synthetic resorbable hydroxyapatite (R-HA) (Osteogen, Impladent) has been introduced for bone repair[11–13] and sinus floor augmentation.[8,14–17] This nonceramic material, composed of a cluster of small crystals with relatively low microstructure porosity, is presumably osteoconductive, with a mineral reservoir that promotes new bone formation.[13] A similar percentage of bone-to-implant contact in the augmented sinus was shown when R-HA was compared to natural bovine hydroxyapatite and to demineralized freeze-dried bone in beagle dogs.[18] No new bone formation around the implants was observed when demineralized freeze-dried bone was applied. However, R-HA was not evaluated
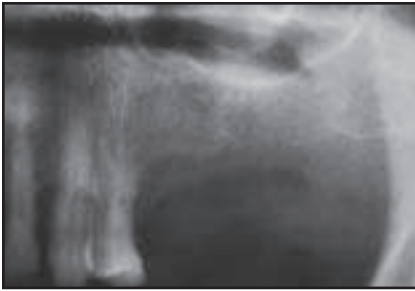
Fig 1a (left) *Preoperative radiograph of the left maxillary region shows 6- to 7-mm bone height of the posterior residual ridge.*

Fig 1b (right) *Postoperative radiograph shows the grafted material completely surrounding the implant bodies.*

Fig 2a *Preoperative radiograph of a posterior atrophic maxilla shows a residual ridge of 1 to 2 mm in height.*
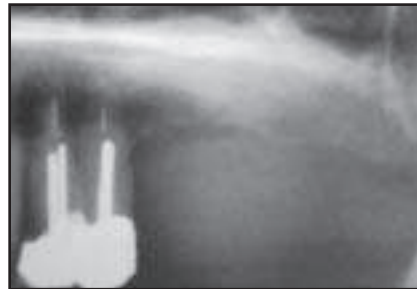
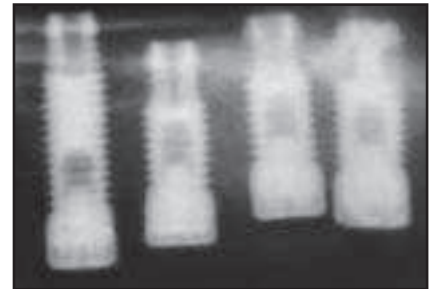**Fig 2b** *Grafted mineral particles are well-confined to the subantral area.*

Fig 2c *Four implants are placed in the augmented site after 6 months.*

morphometrically, and most human studies are based on random clinical cases.

In the present study, 10 consecutive sinus lift procedures were carried out using R-HA as an augmentation material. The histopathologic healing pattern of these sites was examined at 12 months. A morphometric analysis was performed in all sites at the lateral and deep augmented areas. The mean newly formed bone and lamellar:woven bone ratios were measured in these sites using polarizing microscopy.

Method and materials

Ten healthy patients (five women and five men ranging in age from 36 to 66 years) with no systemic disorders, who were to receive posterior implant-supported fixed prostheses, participated in the study. The diagnostic radiographs revealed atrophic posterior maxillae. In all patients, the pneumatized sinus space and resorbed alveolar bone resulted in a residual ridge height of 1 to 7 mm. R-HA was used as the augmentation material in the sinus lift procedure. In

eight patients, where the residual ridge height was 4 to 7 mm (Fig 1a), simultaneous augmentation and implant placement were carried out (Fig 1b). A staged procedure was preferred (Figs 2a and 2b) where the residual ridge height was 1 to 3 mm. In these two patients, implants were placed 6 months after the augmentation procedure (Fig 2c). All implants were root form, 3.7 to 4.5 mm in diameter, and 10 to 15 mm in length.
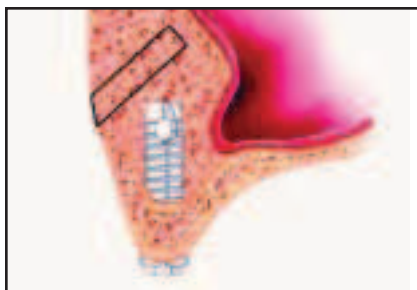
Fig 3a (left) *Harvesting of specimen core sample.*

Fig 3b (right) *Approximately 10 mm cylindric bone sample is harvested by the trephine bur before the specimen fixation process.*

Surgical procedures

Patients were premedicated with Ketoprofen (Ketonal, Agis Industries) 100 mg. One hour before surgery, buccal and palatal local anesthesia was administered using lidocaine HCl 3% and 1:80,000 norepinephrine by slow infiltration. Initially, sequential step-up cutting burs were used to prepare implant osteotomy sites at the residual available ridge areas. The lateral fractured sinus wall technique, originally described by Boyne and James[19] and Tatum,[20] was then performed. An extensive buccal flap was reflected, exposing the lateral external sinus bony wall. Oval/rectangular window boundaries were demarcated (mean 10 mm × 16 mm) with a 2-mm round diamond bur according to osseous topography and with the aid of panoramic radiographs and computerized tomographic (CT) scans. A periodontal probe was used to measure window size and distance from the residual bony crest to the inferior window border for second-stage surgical procedures. After the inward-upward loosening of the lateral bony wall window, the Schneiderian membrane was carefully reflected from its lower adherence with a broad, flat curette. R-HA particles, 300 to 400 µm, were soaked with venous blood and carried into the sinus space with a bone-grafting syringe (Bio-Interfaces) in two increments. In between, the implant osteotomy site was completed into the established augmented space, followed by implant placement. The second increment of the grafted mineral was then added to obturate the surgical sinus window. Finally, a resorbable, bilayer, porcine collagen membrane (BioGide, Osteohealth) was applied over the entire area. Soft tissue closure was achieved with a nonabsorbable polyviolene suture (4-0; Look, Surgical Speciality).

In the two patients where a staged approach was used, implants were placed after 6 months. Postoperative systemic antibiotics of 500 mg amoxicillin (Moxypen Forte, Teva Pharmaceutical Industries) three times a day for 1 week and 275 mg naproxen (Narocin, Teva Pharmaceutical Industries; two-tablet initial dose, thereafter one tablet every 6 to 8 hours as needed) were prescribed. A 0.2% chlorhexidine gluconate mouthwash (Tarodent, Taro Pharmaceutical Industries) was used for 45 seconds, twice daily for 2 weeks. Sutures were removed after 14 days.

At the implant uncovering phase, the buccal soft tissue flap was further elevated to the previous window area for hard tissue retrieval using a 2.5-mm-internal-diameter trephine bur. Bone was harvested with careful orientation with the current position of the implant body. The trephine bur was drilled through the previous lateral window frame and between the apical end of the implants, in a diagonal, superior, upward direction toward the new location of the Schneiderian membrane (Fig 3a). Thus, the harvesting procedure would not affect or compromise the implants. Cylindric specimens, 7 to 8 mm long (Fig 3b), were marked to identify the lateral and deep ends for further orientation.
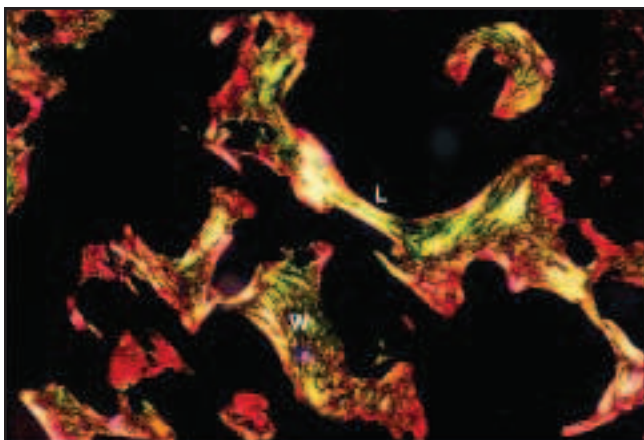
Fig 4 *Under polarization, woven bone is characterized by a greenish-yellow-orange, unorganized pattern (W). The organized lamellar bone is characterized by its thick, greenish-yellow strips (L) (picrosirius red stain; original magnification × 400).*
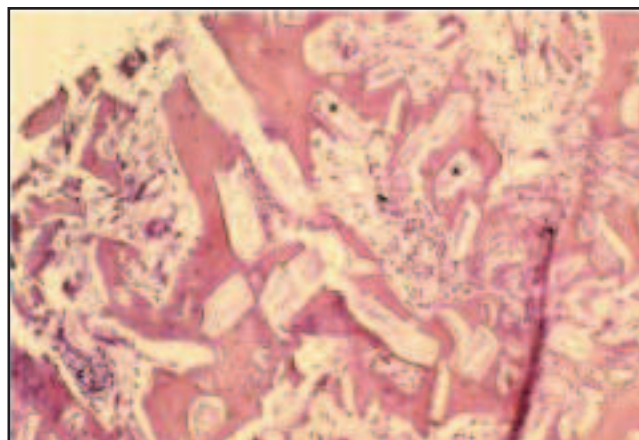

Fig 5 *Rectangular R-HA particles (*) are primarily surrounded by newly formed bone in different stages of maturation (hematoxylin-eosin stain; original magnification × 100).*
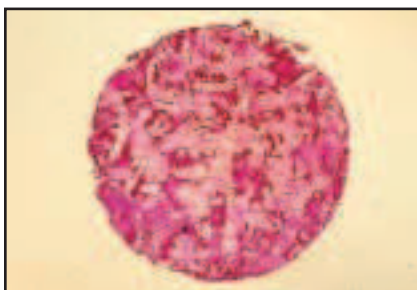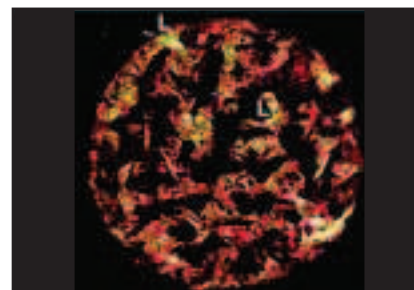

Fig 6a (left) *Photomicrograph of a specimen core section. Newly formed bone surrounds R-HA empty lacunae, comprised of an amorphous mass (picrosirius red stain; original magnification × 20).*

Fig 6b (right) *Polarization of Fig 6a shows R-HA particles surrounded mainly by woven bone and occasionally by lamellar bone (L).*

Histologic preparation

Cylindric specimen cores were fixed in 10% neutral buffered formalin for 1 week and then decalcified with 5% formic acid for an additional 2 weeks. Serial transverse sections of the paraffin-embedded specimens, 5 µm in width, were prepared using a microtome. The slides were stained with hematoxylin-eosin and picrosirius red for polarizing microscopy. Picrosirius red–stained serial slides were examined with polarizing microscopy specific for collagen,[21] and the area fraction of woven and lamellar bone was measured and compared in the lateral and deep specimen areas.

Photomicrographs (20×) of each picrosirius red–stained section were taken using an automatic camera (Olympus C35AD-4) connected to a microscope (Olympus BH-2) with polarized light. Woven bone was recognized by its random, unorganized fibrillar pattern, usually with polarization colors ranging from greenish-yellow to yellow-orange, depending on fiber width (Fig 4).

Thick strips of greenish-yellow colors in an organized pattern characterized the lamellar bone. R-HA mineral particles appeared as a dark area.

The point-counting technique[22,23] was used for area fraction estimation. A 64-square (1.5 cm × 1.5 cm) graticule was superimposed on 13 cm × 18 cm illustrations. Each graticule-square center was marked with a +. Whenever the graticule-square center hit one of the bone types, the specified type scored one point. The area fraction of each bone type was calculated as previously

described[23–26] at both core ends of the 10 specimen cores. Measurements of area fraction were carried out on serial sections mounted on slides. Each histologic slide contained 10 to 12 sections. Every fifth slide was examined morphometrically. Since the width of each section was 5 µm, the thickness of the external/peripheral specimen core examined was approximately 750 µm (slides 5, 10, and 15) and assumed to be the mean lateral area. Slides 60, 65, and 70, ie, the 750-µm-thick internal end, were examined to give the deep area mean.

Statistical analysis was carried out using analysis of variance (ANOVA) with repeated measures (BMDP Statistical Software).

Table 1	Percentage of bone area fraction and lamellar:woven bone ratio of the 10 specimens			
	Lateral sections		**Deep sections**	
Specimen	**% of bone area fraction**	**Lamellar:woven bone ratio**	**% of bone area fraction**	**Lamellar:woven bone ratio**
1	31.0	0.13	53.0	0.29
2	24.3	0.13	39.1	0.28
3	22.9	0.07	30.2	0.37
4	37.5	0.07	34.2	0.12
5	22.3	0.23	31.9	0.37
6	28.7	0.17	43.8	0.23
7	22.6	0.17	36.3	0.19
8	28.5	0.16	39.5	0.20
9	24.6	0.13	33.2	0.35
10	38.9	0.25	37.5	0.35
Mean	28.1	0.15	37.8	0.27
SD	6.7	0.06	9.1	0.08

SD = standard deviation.

Results

Radiographically, the mineral material filled the sinus area and surrounded the implants (Figs 1b and 2c). In the two-stage procedure, the augmented site was well-defined, apart from the remaining diminished antrum (Fig 2b). During implant placement, bone had a solid appearance and was routinely drilled by step-up cutting burs. Healing was uneventful, and no complaints were reported 2 to 3 weeks postsurgery. All 36 implants were clinically integrated at the time of prosthetic superstructure connection. At 12 months, during healing abutment placement, all implants were stable and no sign of crestal bone resorption was evident. The augmented buccal area was solid and seldom distinguished from the neighboring original osseous wall.

Histologically, bone formation was evident in all specimen cores. Rectangular R-HA particles, in various sizes, were surrounded by newly formed bone (Fig 5). Bone deposition was evident around the mineral crystals. However, no osteoblasts were identified in the interface zone between the grafted particles and osseous tissue margins. Some particles, although rare, were surrounded by fibrous encapsulation. Most particles, which underwent the decalcification process during histologic preparation, harbored an amorphous mass within their spaces (Fig 6a). Under polarized microscopy, picrosirius red–stained slides showed mainly woven bone and, to a lesser degree, lamellar bone (Fig 6b). This polarization, ie, total blackness, also refuted the existence of collagen within the noted amorphous mass.

Morphometrically, mean bone area fraction at the lateral side of the 10 specimens was 28.1%, ranging between 22.3% and 38.9%

(standard deviation [SD] 6.7), and increasing at the deep area to 37.8%, ranging between 30.2% and 53.0% (SD 9.1) (Table 1). Differences were statistically significant (*P* < .001). Under polarization of the picrosirius red–stained slides, mean lamellar:woven bone ratio at the lateral/external side was 0.15 (1:7.2), ranging between 0.07 and 0.25 (SD 0.06); at the deep end, it was 0.27 (1:4.2), ranging between 0.12 and 0.37 (SD 0.08). Differences were statistically significant (*P* < .001). No correlation was observed between bone area percentage and lamellar:woven bone ratio (correlation coefficient test).

Discussion

R-HA, a microporous, nonceramic alloplast that resorbs slowly over time, has been used successfully for periodontal treatment,[12] osseous repair,[11,13] and sinus lift procedures.[8,14–17] Physiochemically and crystallographically, it is equivalent to human bone. In vitro, R-HA has shown biocompatibility by supporting cell growth and fibroblast metabolism, including collagen production. It is also superior to ceramic hydroxyapatite in cell viability percentage, thus proving biologically and physically to be an appropriate alloplast material.[27] A three-dimensional configuration of R-HA provides more space between particles when nonceramic R-HA is compared to ceramic hydroxyapatite by their structures. These spaces could facilitate cellular and tissue proliferation within the grafted material, thus enhancing faster osseointegration[27]; however, in vivo studies do not always confirm in vitro studies.

What is important is the implant success rate over time. A 98% cumulative success rate over 5 years has been found with pure alloplasts,[5] similar to that reported with R-HA.[17] However, better results were obtained with the two-stage approach when simultaneous implant placement was compared to delayed placement.[8] In the present study, all implants were successful. A one-stage procedure was not carried out in an atrophic residual ridge of less than 3 mm in height. In a sinus consensus report,[5] four of 163 implants failed during the first year, ie, before

loading. Therefore, in the present study, the predictable 12-month success rate of implant integration to the augmented sinus could be stable and valid for the long term, depending on the type of augmentation material used.

Follow-up radiographs of the 10 sites disclosed the relative opacity of the augmented area occupied by the mineral. The diminished radiolucent sinus space was clearly distinguishable from the augmented site. Where the two-stage approach was used, the implant osteotomy site was prepared through solid, hard, condensed tissue.

Histologically, R-HA particles were evident in all specimen core sections. While bone and marrow tissue varied in quantity, the mineral particles maintained their captured areas. Although elongated cubiod cells, ie, osteoblasts, were not seen between the mineral clusters and the deposited bone, the particles were surrounded primarily by new bone in different stages of maturation. However, although rarely observed, fibrous encapsulation of some grafted particles could not be ruled out. The dominant presence of the R-HA particles in the augmented sites at 12 months also showed that these particles serve as a long-term mineral reservoir.

A significant difference between the osseous tissue percentage at the lateral and deep ends of the 10 specimens was shown when the point-counting technique was used.[22,23] The lateral/external area, which was covered by a biologic barrier membrane, probably suffered from lack of

nourishment at the early stage of healing. Micromovements could also be a determinant factor.[28] The deep areas received nourishment from the Schneiderian membrane as well as from the neighboring osseous walls, which could partially explain the higher osseous area fraction at the deep side compared to the lateral one. Likewise, when analyzing the lamellar:woven bone ratio in a sinus augmented by demineralized bone matrix,[29] lamellar bone was noted near the maxillary host bone, whereas woven bone was in the vicinity of the grafted material. Since fewer R-HA particles were present at the deeper areas, this could also explain the increase of lamellar bone at the deep augmented site. Woven bone always precedes lamellar bone in the course of ossification and is recognized by an unorganized morphology of collagen fibers.[30] Lamellar bone is featured in concentric layers containing collagen in organized parallel arrays.

Both bone types can be distinguished with polarizing lenses. Picrosirius red–stained slides under polarized-light microscopy demonstrated differences in polarization colors of collagen fibers in different samples. The color profile is related to the physical aggregation of collagen. Green to green-yellow corresponds to poorly organized collagen fibers, whereas an orange-reddish color corresponds to well-packed fibers.[21,31] The shift from green to reddish color indicates an increase of physical aggregation of collagen fibers and a higher degree of ordering in the remodeling process. Since deposition and mineralization occur faster in woven bone, the difference in lamellar:woven bone ratio at the lateral and deep sides indicates that the maturation process occurred from a central to peripheral direction. However, in the present study, most of the examined sections consisted of woven bone, indicating the delayed remodeling process of lamellar bone.[32]

Covering the augmented sinus site by a biologic barrier membrane is a well-documented treatment.[33,34] The membrane promotes corticalization and maturation[35] at the previously removed lateral bony wall of the sinus.

As a filler material, R-HA exhibited biocompatibility and osteoconductivity in sinus augmentation procedures. Bone area fraction and remodeling (ie, osseous lamellar arrangement) increased in a lateral/deep direction toward the vicinity of the Schneiderian membrane. Immediate or delayed implant placement in this augmented site resulted in successful osseointegration in a predictable manner.

Acknowledgments

References

1. Smiler DG, Holmes RE. Sinus lift procedures using porous hydroxyapatite: A preliminary clinical report. J Oral Implantol 1987;13:239–253.

2. Chanavaz M. Maxillary sinus: Anatomy, physiology, surgery, and bone grafting related to implantology—Eleven years of surgical experience (1979–1990). J Oral Implantol 1990;16:199–209.

3. Wheeler SL, Holmes RE, Calhoun CJ. Six-year clinical and histologic study of sinus-lift grafts. Int J Oral Maxillofac Implants 1996;11:26–34.

4. Boyne PJ, Marx RE, Nevins M, et al. A feasibility study evaluating rhBMP-2/absorbable collagen sponge for maxillary sinus floor augmentation. Int J Periodontics Restorative Dent 1997;17: 11–25.

5. Jenson OT, Shulman LB, Block MS, Iacono VJ. Report of the sinus consensus conference of 1996. Int J Oral Maxillofac Implants 1998;13(suppl):11–45.

6. Kirsch A, Ackermann KL, Hürzeler MB, Hutmacher D. Sinus grafting with porous hydroxyapatite. In: Jensen OT (ed). The Sinus Bone Graft. Chicago: Quintessence, 1999:79–84.

7. Misch CE. The maxillary sinus lift and sinus graft surgery. In: Contemporary Implant Dentistry. St Louis: Mosby, 1999:469–495.

8. Smiler DG, Johnson PW, Lozada JL, et al. Sinus lift grafts and endosseous implants: Treatment of the atrophic posterior maxilla. Dent Clin North Am 1992;36: 151–186.

9. Wheeler SL. Sinus augmentation for dental implants: The use of allograft materials. J Oral Maxillofac Surg 1997;55: 1287–1293.

10. Misch CE. Bone augmentation for implant placement: Keys to bone grafting. In: Contemporary Implant Dentistry. St Louis: Mosby, 1999:451–467.

11. Wagner JR. Clinical and histological case study using resorbable hydroxylapatite for the repair of osseous defects prior to endosseous implant surgery. J Oral Implantol 1989;15:186–192.

12. Corsair A. A clinical evaluation of resorbable hydroxylapatite for the repair of human intra-osseous defects. J Oral Implantol 1990;16:125–128.

13. Ricci JL, Blumenthal NC, Spivak JM, Alexander H. Evaluation of a low-temperature calcium phosphate particulate implant material: Physical-chemical properties and in vivo bone response. J Oral Maxillofac Surg 1992;50:969–978.

14. Whittaker JM, James RA, Lozada J, Cordova C, GaRey DJ. Histological response and clinical evaluation of heterograft and allograft materials in the elevation of the maxillary sinus for the preparation of endosteal dental implant sites. Simultaneous sinus elevation and root form implantation: An eight-month autopsy report. J Oral Implantol 1989;15: 141–144.

15. Wagner JR. A $3^1/_2$-year clinical evaluation of resorbable hydroxylapatite OsteoGen (HA Resorb) used for sinus lift augmentation in conjunction with the insertion of endosseous implants. J Oral Implantol 1991;17:152–164.

16. Vlassis JM, Hürzeler MB, Quiñones CR. Sinus lift augmentation to facilitate placement of nonsubmerged implants: A clinical and histological report. Pract Periodontics Aesthet Dent 1993;5:15–23.

17. Fugazzotto PA, Vlassis J. Long-term success of sinus augmentation using various surgical approaches and grafting materials. Int J Oral Maxillofac Implants 1998; 13:52–58.

18. Wetzel AC, Stich H, Caffesse RG. Bone apposition onto oral implants in the sinus area filled with different grafting materials. A histological study in beagle dogs. Clin Oral Implants Res 1995;6:155–163.

19. Boyne PJ, James RA. Grafting of the maxillary sinus floor with autogenous marrow and bone. J Oral Surg 1980;38:613–616.

20. Tatum H Jr. Maxillary and sinus implant reconstructions. Dent Clin North Am 1986;30:207–229.

21. Dayan D, Hiss Y, Hirshberg A, Bubis JJ, Wolman M. Are the polarization colors of picrosirius red-stained collagen determined only by the diameter of the fibers? Histochemistry 1989;93:27–29.

22. Chalky HW. Method for quantitative morphologic analysis of tissues. Natl Cancer Inst 1943;4:47–53.

23. Bellhouse DR. Area estimation by point counting techniques. Biometrics 1981;37: 303–312.

24. Dayan D, Bodner L, Horowitz I. Effect of salivary hypofunction on the healing of extraction wounds: A histomorphometric study in rats. J Oral Maxillofac Surg 1992; 50:354–358.

25. Artzi Z, Tal H, Dayan D. Porous bovine bone mineral in healing of human extraction sockets. Part 1. Histomorphometric evaluation at 9 months. J Periodontol 2000;71:1015–1023.

26. Artzi Z, Tal H, Dayan D. Porous bovine bone mineral in healing of human extraction sockets. Part 2. Histochemical observations at 9 months. J Periodontol 2001; 72:152–159.

27. Ruano R, Jaeger RG, Jaeger MMM. Effect of a ceramic and a non-ceramic hydroxyapatite on cell growth and procollagen synthesis of cultured human gingival fibroblasts. J Periodontol 2000;71: 540–545.

28. Wikesjö UM, Nilvéus R. Periodontal repair in dogs: Effect of wound stabilization on healing. J Periodontol 1990;61:719–724.

29. Groeneveld EH, van den Bergh JP, Holzmann P, ten Bruggenkate CM, Tuinzing DB, Burger EH. Mineralization processes in demineralized bone matrix grafts in human maxillary sinus floor elevations. J Biomed Mater Res 1999;48: 393–402.

30. Juan R. Tumors and tumor-like conditions of bone. In: Kissane JM (ed). Anderson's Pathology, ed 8. St Louis: Mosby, 1985: 1778–1816.

31. Dayan D, Waner T, Tal H, Nyska A. Polarizing microscopy of picrosirius red-stained collagen from oxodipine-induced hyperplastic gingiva in beagle dogs. Int J Exp Pathol 1993;74:225–228.

32. Gorski JP. Is all bone the same? Distinctive distributions and properties of non-collagenous matrix proteins in lamellar vs woven bone imply the existence of different underlying osteogenic mechanisms. Crit Rev Oral Biol Med 1998;9: 201–223.

33. Avera SP, Stampley WA, McAllister BS. Histologic and clinical observations of resorbable and nonresorbable barrier membranes used in maxillary sinus graft containment. Int J Oral Maxillofac Implants 1997;12:88–94.

34. Tarnow DP, Wallace SS, Froum SJ, Rohrer MD, Cho S-C. Histologic and clinical comparison of bilateral sinus floor elevations with and without barrier membrane placement in 12 patients: Part 3 of an ongoing prospective study. Int J Periodontics Restorative Dent 2000;20:116–125.

35. Ohnishi H, Fujii N, Futami T, Taguchi N, Kusakari H, Maeda T. A histochemical investigation of the bone formation process by guided bone regeneration in rat jaws. Effect of PTFE membrane application periods on newly formed bone. J Periodontol 2000;7:341–352.